Letter

Full counting statistics of interacting lattice gases after an expansion: The role of condensate depletion in many-body coherence

Gaétan Hercé,* Jan-Philipp Bureik,* Antoine Ténart, Alain Aspect, Alexandre Dareau, and David Clément
Université Paris-Saclay, Institut d'Optique Graduate School, Centre National de la Recherche Scientifique, Laboratoire Charles Fabry, 91127 Palaiseau, France

(Received 29 July 2022; accepted 6 February 2023; published 17 March 2023)

We study the full counting statistics (FCS) of quantum gases in samples of thousands of interacting bosons, detected atom by atom after a long free-fall expansion. In this far-field configuration, the FCS reveals the many-body coherence from which we characterize iconic states of interacting lattice bosons by deducing their normalized correlations $g^{(n)}(0)$ up to the order $n = 6$. In Mott insulators, we find a thermal FCS characterized by perfectly contrasted correlations $g^{(n)}(0) = n!$. In interacting Bose superfluids, we observe small deviations to the Poisson FCS and to the ideal values $g^{(n)}(0) = 1$ expected for a pure condensate. These deviations become larger as we increase the interaction strength and reveal the role of the quantum depletion of the condensate on many-body coherence. The approach to many-body correlations demonstrated here is readily extendable to characterize a large variety of interacting quantum states and phase transitions.

DOI: 10.1103/PhysRevResearch.5.L012037

The dispersion of a physical quantity contains important information, beyond that obtained from its average value. The analysis of quantum and thermal noise is central in various systems, ranging from quantum electronics [1] and quantum optics [2] to quantum gases [3–5]. The ultimate precision on the measurement of noise is given by the full counting statistics (FCS) [6], which is obtained with single-particle-resolved detection methods that provide the number of particles detected in a given time and/or space interval. These methods yield high-order moments of the particle number beyond the variance. Probing high-order moments is a means to study quantum phase transitions [7–9], universality [10,11], entanglement properties [12], or out-of-equilibrium dynamics [13]. The FCS has successfully characterized various phenomena in mesoscopic conductors [1,6,14,15] and Rydberg [16–18] and noninteracting [19,20] atomic gases.

From a quantum information perspective, the FCS holds great promise for large ensembles of particles. In contrast to a full-state tomography [21], the FCS is accessible even in large systems as it probes information only about the diagonal part of the n-body density matrices, i.e., populations. Although it does not contain the total information about the quantum state, the FCS is sufficient to identify many quantum states without resorting to a consuming tomography. A similar idea was introduced by Glauber to characterize light sources from photon correlations at any order [22]. For Gaussian states, for which the Wigner function is positive [2], measuring the FCS or the magnitudes of correlation functions is indeed equivalent.

In strongly correlated quantum states characterized by non-Gaussian Wigner functions, measuring the FCS and many-body correlations is expected to reveal the nontrivial nature of such states [5,23–25]. Moreover, recent works have shown that applying random unitary transformations before measuring the FCS provides access to nondiagonal correlators [26,27], further motivating the development of experimental approaches to the FCS in strongly interacting quantum systems.

In this Letter, we report the measurement of the full counting statistics in large three-dimensional (3D) ensembles ($\approx 5 \times 10^3$ atoms) of interacting lattice bosons after a free-fall expansion [see Fig. 1(a)]. The FCS is obtained from the statistics (over many experimental runs) of the atom number N_Ω falling in small volumes V_Ω (see below). This allows us to extract two quantities of interest, the probability distribution $P(N_\Omega)$ and the magnitudes $g^{(n)}(0)$ of n-body correlation functions. We measure these quantities in a configuration analogous to the far-field regime of light propagation during which interferences take place, and after which the FCS identifies quantum states through their many-body coherence [28].

In quantum gases, far-field—or momentum—correlations have been measured with single-atom detection in noninteracting and nondegenerate bosonic [29,30] and fermionic [31,32] gases and in Bose-Einstein condensates (BECs) [33]. More recently momentum correlations in interacting bosons [34–36] and interacting fermions [37] were studied. However, high-order correlations have thus far been measured only in one-dimensional (1D) noninteracting bosons [30]. Here, we study various regimes of interacting 3D lattice bosons across the superfluid-to-Mott transition, extending the measurement of many-body correlations to the strongly interacting regime. This allows us to reveal the role of the depletion of the condensate in the coherence properties of interacting Bose superfluids.

*These authors contributed equally to this work.

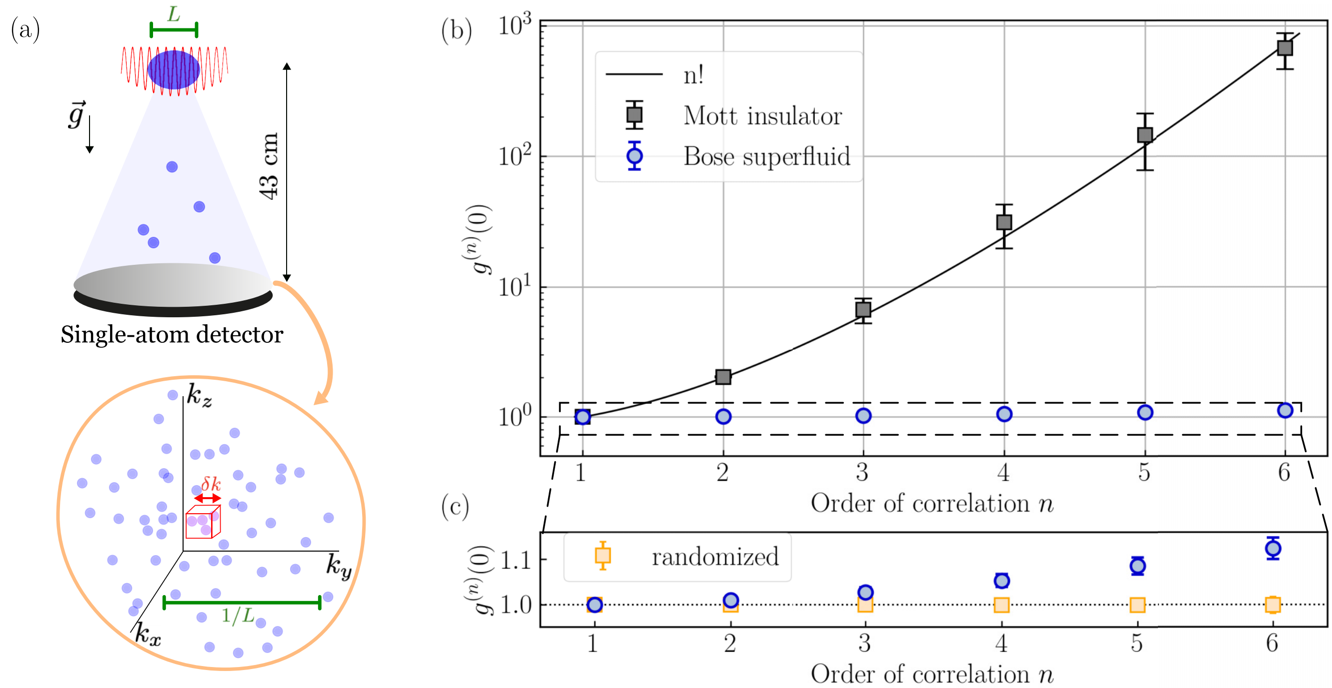

FIG. 1. (a) Free-fall expansion of interacting quantum gases of metastable helium-4 atoms from a three-dimensional optical lattice, yielding the 3D positions of individual atoms in momentum space. The FCS describes the statistics of the atom number N_Ω detected in a voxel of volume $V_\Omega \sim (\delta k)^3$ (red cube). To reveal the many-body coherence properties of the trapped gas of size L, δk is chosen such that $\delta k \ll 2\pi/L$. (b) Magnitudes $g^{(n)}(\mathbf{0})$ of n-body correlations as a function of the order n, measured in a Mott insulator (black squares) and a superfluid (blue circles). The black solid line is the prediction for thermal states, $g^{(n)}(0) = n!$. (c) $g^{(n)}(\mathbf{0})$ in the superfluid (blue circles) and in a randomized set (orange squares, see main text). A deviation from the prediction for a pure coherent state, $g^{(n)}(0) = 1$, is observed.

Bose-Einstein condensation is associated with the breaking of a phase symmetry [38] whose complex order parameter defines a coherent state describing the BEC. Coherent states have a Poisson counting statistics, $P(N_\Omega) = \langle N_\Omega\rangle^{N_\Omega} \exp[-\langle N_\Omega\rangle]/N_\Omega!$ where N_Ω is the number of detected bosons in the considered volume V_Ω, and a full coherence $g^{(n)} = 1$ at any order n of normalized correlations [22]. The equilibrium state of trapped noninteracting bosons at zero temperature is a pure BEC, described by such a coherent state. In an ensemble of interacting bosons, the BEC is depleted by the quantum depletion, whose momentum-space FCS is not that of a coherent state. The quantum depletion is indeed a superposition of two-mode squeezed states at opposite momenta [36] with a thermal-like statistics in small volumes of the momentum space [35]. The FCS of an interacting Bose superfluid, i.e., a superposition of a BEC and of the quantum depletion, can thus be expected to deviate from that of a perfect coherent state. Similar modifications to the properties of pure BECs are expected at finite temperature due to the thermal depletion. A central result of our Letter is to reveal these deviations, which had not been observed previously [33], in our experiment.

We probe quantum gases of metastable helium-4 atoms (^{4}He*) adiabatically loaded in the lowest energy band of a 3D optical lattice [39]. The lattice implements the 3D Bose-Hubbard Hamiltonian whose main parameters are the tunneling amplitude J and the on-site (repulsive) interaction U. Our measurement of the FCS in the far field exploits the 3D atom-by-atom detection of ^{4}He* after a long free-fall expansion [40,41] [see Fig. 1(a)]. A crucial asset of our Letter is the ability to probe many-body coherence in volumes smaller than the one occupied by one mode in momentum space, i.e., $V_\Omega \ll (2\pi/L)^3$ with L the in-trap size of the gas. This possibility is given by the large quantum efficiency of our detector [$\eta = 0.53(2)$] [36]. From the statistics of the atom number N_Ω falling in small voxels V_Ω, we measure the probability distribution $P(N_\Omega)$ of N_Ω and the magnitudes $g^{(n)}(0)$ of correlation functions:

$$g^{(n)}(0) = g^{(n)}(\boldsymbol{k}, \boldsymbol{k}, \dots, \boldsymbol{k}) = \frac{\langle [a^\dagger(\boldsymbol{k})]^n [a(\boldsymbol{k})]^n \rangle}{\langle a^\dagger(\boldsymbol{k}) a(\boldsymbol{k})\rangle^n}, \quad (1)$$

where $\boldsymbol{k}$ is the momentum where the volume V_Ω is located. We determine the magnitudes $g^{(n)}(0)$ (up to $n = 6$) from the factorial moments of N_Ω [42],

$$g^{(n)}(0) = \frac{\langle N_\Omega(N_\Omega - 1)\dots(N_\Omega - n + 1)\rangle}{\langle N_\Omega\rangle^n}, \quad (2)$$

transposing a well-known approach in quantum optics [43]. As shown in Fig. 1(b) and discussed below, $g^{(n)}(0)$ is found to vary by several orders of magnitude between the superfluid and the Mott insulator regimes.

We first investigate the many-body coherence of Mott insulators. A "perfect" Mott insulator—a uniform Mott insulator at zero temperature—is thought of as a Fock state in the (in-trap) position basis. In the momentum basis, it exhibits thermal statistics [34,44,45]. Thermal states are characterized by a counting statistics $P(N_\Omega) = (1-q)q^{N_\Omega}$ where $q = \langle N_\Omega\rangle/1 + \langle N_\Omega\rangle$ and $g^{(n)}(\boldsymbol{k}, \boldsymbol{k}, \dots, \boldsymbol{k}) = n!$ [46]. Note that the probability distributions $P(N_\Omega)$ for Gaussian states—

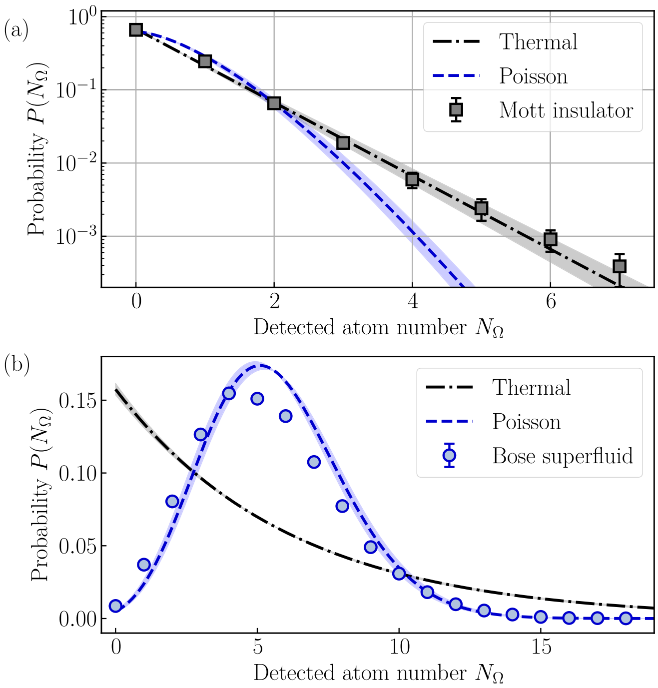

FIG. 2. (a) Probability distribution $P(N_\Omega)$ to find N_Ω atoms in a volume V_Ω when probing a Mott insulator with unity filling (black circles). The prediction for thermal (respectively, Poissonian) statistics is shown as a dash-dotted black (respectively, dashed blue) line using the measured value $\langle N_\Omega \rangle = 0.46(5)$. The shaded areas reflect the uncertainty on $\langle N_\Omega \rangle$. (b) Same as panel (a) in the mode $\boldsymbol{k} = \boldsymbol{0}$ of lattice superfluids with $U/J = 5$ with $\langle N_\Omega \rangle = 5.3(2)$. Error bars are smaller than the dots.

such as those with a thermal or a Poisson FCS—are fully determined by a single parameter, the average number $\langle N_\Omega \rangle$ [2]. Therefore, a detection efficiency η smaller than 1 does not affect their measurement—nor that of $g^{(n)}$. We realize Mott insulators with $N = 6.5(6) \times 10^3$ atoms at $U/J = 76$, which corresponds to a lattice filling of one atom per site at the trap center [34]. To compute the counting statistics, we divide the first Brillouin zone into cubic voxels V_Ω of size $\delta k = 6 \times 10^{-2} k_d$ and average the probability distributions measured over all these voxels. Here $k_d = 2\pi/d$ is the momentum associated with the lattice spacing $d = 775$ nm and the size δk is comparable to that of one mode in momentum space, $\delta k \sim 2\pi/L$ (see Supplemental Material [47]). The resulting distribution $P(N_\Omega)$ in the Mott state is shown in Fig. 2(a). It is found to be in excellent agreement with a thermal statistics whose average atom number is that measured in the experiment, $\langle N_\Omega \rangle = 0.46(5)$.

The properties of the Mott state are also revealed through the magnitudes $g^{(n)}(0)$ of the correlation functions. Fully contrasted correlation functions are measured only when computed in voxels of small size $\delta k \ll 2\pi/L$, a requirement which is more stringent than the one for measuring $P(N_\Omega)$ [47]. The magnitudes $g^{(n)}(0)$ are plotted in Fig. 1(b) and are found in excellent quantitative agreement with the prediction for thermal states, $g^{(n)}(0) = n!$. They represent a significant progress with respect to the literature where only two- [44] and three-body [34] correlations had been measured with limited amplitudes $g^{(n)}(0) < n!$.

In a second set of experiments, we address the n-body coherence of interacting Bose superfluids. We produce lattice superfluids with $N = 5(1) \times 10^3$ at $U/J = 5$. In momentum space, the BEC occupies a volume of width $\Delta k \simeq 0.15 k_d$ centered at $\boldsymbol{k} = \boldsymbol{0}$ [36]. The statistics of the atom number falling in a sphere S_Ω of a radius $\delta k = 0.025 k_d \ll \Delta k$, centered at $\boldsymbol{k} = \boldsymbol{0}$, is sufficient to extract the counting statistics [47]. The volume of S_Ω is chosen much smaller than the one occupied by the condensate to circumvent the macroscopic constraint of the fixed total atom number N on the measured statistics of N_Ω [47]. In Fig. 2(b), we plot the corresponding probability distribution $P(N_\Omega)$, which is found to be close to the Poisson FCS and which clearly differs from the thermal FCS. This is confirmed by the measured values of $g^{(n)}(0) \approx 1$ at any order n in the BEC mode [see Fig. 1(b)]. These results, predicted by Glauber for a coherent state, are in striking contrast with those of the Mott state, a difference that illustrates the outstanding capabilities of the FCS to reveal the n-body coherence when measured after an expansion.

Interestingly, however, our measurements in the BEC mode deviate from the predictions for a coherent state and from a previous observation [33]: the deviation in the FCS [see Fig. 2(b)] is reflected in the fact that $g^{(n)}(0) > 1$, as shown in Fig. 1(c). To verify that the observed deviations are statistically meaningful, we apply our computation of the n-body correlations to a randomized set, with the same numbers of atoms and of runs. This randomized set is obtained by randomly shuffling the detected atoms across the experimental runs. Doing so, atom correlations present within individual runs, i.e., before shuffling, should vanish, and a Poisson statistics is expected as a result of the discrete nature of our detection method applied to fully independent events. Indeed we find $g^{(n)}(0) = 1.00(2)$ at any order n [see the orange squares in Fig. 1(c)], confirming that the deviations in the (nonrandomized) experimental data are significant. The randomization method also yields a Poisson statistics when applied to the Mott insulator data set. Note that the results of the randomization method validate the algorithm used to compute the n-body correlations and provide a means to test the accuracy of the measured statistics [47].

As discussed previously, deviations to a perfectly coherent state are expected in the presence of quantum and/or thermal depletion of the condensate. Here, we probe Bose superfluids with both a quantum and a thermal depletion as our experiment is performed with interacting bosons at finite temperature. In addition, both the BEC and its depletion contribute to the mode $\mathbf{k} = \mathbf{0}$ since atoms are released from a harmonic trap. We are therefore inclined to attribute the observed deviations $g^{(n)}(0) > 1$ to the condensate depletion. To confirm this hypothesis, we repeat our measurements at increasing values of the condensate depletion. We vary the lattice depth to obtain ratios U/J ranging from $U/J = 2$ to 22. In this range of parameters, the gas remains far from entering the Mott insulator regime [39], but it enters the strongly interacting regime where the condensate is strongly depleted (at $U/J = 22$ the condensate fraction is $f_c \approx 0.15$). Importantly, we increase U/J at a constant reduced temperature T/J [39] so that the increase in the condensate depletion is mostly due to an increase of the quantum depletion. In Fig. 3(b) we plot the magnitudes of n-body correlations for $U/J = 20$.

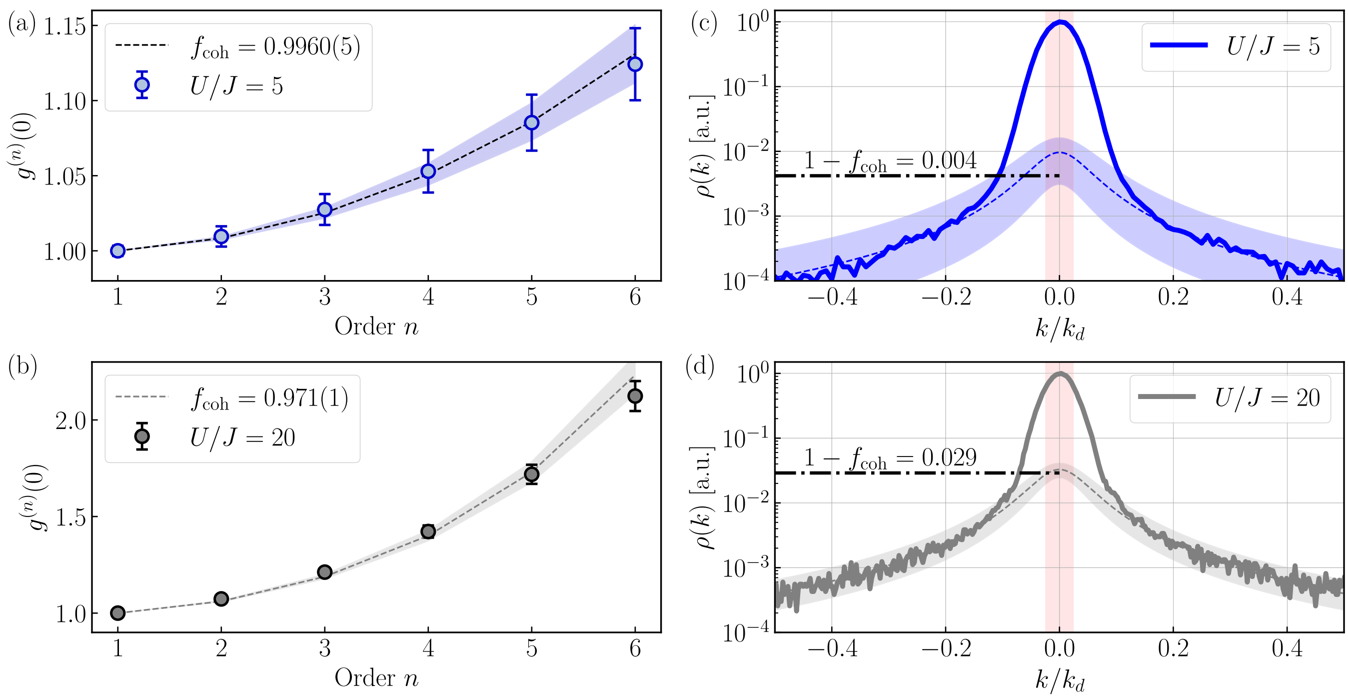

FIG. 3. (a, b) Plots of $g^{(n)}(0)$ measured at $\boldsymbol{k} = \mathbf{0}$ in lattice superfluids with $U/J = 5$ and 20 [data shown in panel (a) are those of Fig. 1(c)]. The dashed lines (respectively, shaded areas) are the predictions of the model with the values $f_{\rm coh}$ (respectively, uncertainties on $f_{\rm coh}$) fitted to the data. (c, d) Plots of 1D cuts through the momentum densities $\rho(k)$ measured at $U/J = 5$ and 20 and normalized to their value at $k = 0$. The vertical shaded area indicates the volume occupied by the sphere S_Ω where the FCS is evaluated. The horizontal dash-dotted lines indicate the fitted values $1 - f_{\rm coh}$ in panels (a) and (b). Lorentzian fits (dashed lines) in the range $[0.2k_d, 0.5k_d]$ estimate the density of the depletion at $k = 0$ (shaded areas represent the fit error).

The deviation from the ideal coherent state is increased, in qualitative agreement with our physical picture.

To be more quantitative, we introduce a heuristic model that describes the contribution of both BEC atoms and depleted atoms to the measured number N_Ω falling in S_Ω. We define the "coherent fraction" $f_{\rm coh}$ as the fraction of N_Ω that belongs to a coherent state BEC. Our model assumes (i) that atoms in the BEC and in the depletion contribute independently to the measured counting statistics in S_Ω [48] and (ii) that the BEC is a coherent state while both the thermal and quantum depletion exhibit thermal statistics in S_Ω. We emphasize that describing the contribution of the quantum depletion with a thermal statistics is an assumption, although the statistics of the quantum depletion was shown to be thermal when measured at *nonzero* momenta, outside the BEC [35]. With the hypotheses of our model, we obtain an analytical prediction for $g^{(n)}(0)$ that depends only on the coherent fraction $f_{\rm coh}$ [47]:

$$g^{(n)}(0) - 1 = \sum_{p=1}^{n-1}\left[(n-p)!\binom{n}{p}^2 - \binom{n}{p}\right] f_{\rm coh}^p (1 - f_{\rm coh})^{n-p}. \tag{3}$$

Note that, while our model straightforwardly predicts the magnitudes $g^{(n)}(0)$, this is not the case for the probability distribution $P(N_\Omega)$ which is difficult to obtain from the moments of N_Ω [49].

In Fig. 3, we fit the data with the analytical prediction of Eq. (3). First, we find that Eq. (3) correctly fits the values of $g^{(n)}(0)$ with a single adjustable parameter $f_{\rm coh}$. Second, the extracted values of $f_{\rm coh}$ decrease with the interaction strength as intuitively expected. The uncertainty on the values $f_{\rm coh}$ is extremely small, at the $\approx$0.1% level. As can be inferred from Fig. 3, the larger the order n of correlations we measure, the smaller the uncertainty on $f_{\rm coh}$. This illustrates the extreme sensitivity of high-order correlations to probe many-body coherence.

A quantitative test of the model would compare the value $1 - f_{\rm coh}$ to the fraction η_D of depleted atoms detected within S_Ω. We are not aware of a quantitative analytical prediction for η_D in 3D interacting trapped lattice Bose gases. However, an indirect comparison is amenable from measuring the momentum densities. In Figs. 3(c) and 3(d), we plot 1D cuts through the momentum densities measured at $U/J = 5$ and 20 and we fit the tails (in the range $[0.2k_d, 0.5k_d]$) with a Lorentzian function to extrapolate the density of the depletion at $k = 0$. Using a Lorentzian function is an arbitrary choice which happens to correctly fit the tails. This analysis indicates that the values $1 - f_{\rm coh}$ are compatible with the extrapolated densities, while both quantities vary by one order of magnitude. Another test of the model is provided in the Supplemental Material [47], supporting the idea which attributes the deviations $g^{(n)}(0) > 1$ to the condensate depletion. It would be interesting to confirm theoretically this picture drawn from the heuristic model, in particular in the strongly interacting regime where the model's hypothesis is uncertain.

In conclusion, we have presented measurements of the full counting statistics and of high-order correlations in interacting lattice Bose gases. We have obtained perfectly contrasted n-body correlations between up to $n = 6$ individual atoms, as illustrated by the measured magnitudes $g^{(n)}(0) \simeq n!$ in Mott insulators. Furthermore, we have shown that the coherence properties of interacting Bose superfluids deviate from those of a coherent state because of the condensate depletion, in particular of the quantum depletion. The role of the depletion in the n-body coherence unveiled in this Letter was not identified previously in the weakly interacting regime [33]. A major technical difference of our experiment with respect to that of [33] is that the volume V_Ω used in that work to compute the statistics is larger than the coherence volume $(2\pi/L)^3$, a choice made in light of a smaller detection efficiency $\eta \approx 0.08$. We conclude that our ability to obtain sufficient statistics in tiny volumes is a major asset to quantitatively probe many-body correlations. In the future, our experimental approach to the full counting statistics could be used to study a large variety of interacting quantum states and phase transitions (see, e.g., [9–11,50]) as well as to access nontrivial n-body correlations [26,27].

We thank S. Butera, A. Browaeys, I. Carusotto, T. Lahaye, T. Roscilde, and the members of the Quantum Gas group at Institut d'Optique for insightful discussions. We acknowledge financial support from the Région Ile-de-France in the framework of the DIM SIRTEQ, the "Fondation d'entreprise iXcore pour la Recherche," the Agence Nationale pour la Recherche (Grants No. ANR-17-CE30-0020-01 and No ANR-22-PETQ-0004). D.C. acknowledges support from the Institut Universitaire de France. A.A. acknowledges support from the Simons Foundation and from Nokia-Bell Labs.

[1] Ya. M. Blanter and M. Büttiker, Shot noise in mesoscopic conductors, Phys. Rep. **336**, 1 (2000).

[2] C. Gardiner and P. Zoller, *Quantum Noise: A Handbook of Markovian and Non-Markovian Quantum Stochastic Methods with Applications to Quantum Optics* (Springer-Verlag, Berlin, 2004).

[3] E. A. Burt, R. W. Ghrist, C. J. Myatt, M. J. Holland, E. A. Cornell, and C. E. Wieman, Coherence, Correlations, and Collisions: What One Learns about Bose-Einstein Condensates from Their Decay, Phys. Rev. Lett. **79**, 337 (1997).

[4] E. Altman, E. Demler, and M. D. Lukin, Probing many-body states of ultracold atoms via noise correlations, Phys. Rev. A **70**, 013603 (2004).

[5] T. Schweigler, V. Kasper, S. Erne, I. Mazets, B. Rauer, F. Cataldini, T. Langen, T. Gasenzer, J. Berges, and J. Schmiedmayer, Experimental characterization of a quantum many-body system via higher-order correlations, Nature (London) **545**, 323 (2017).

[6] L. S. Levitov, H. Lee, and G. B. Lesovik, Electron counting statistics and coherent states of electric current, J. Math. Phys. **37**, 4845 (1996).

[7] D. A. Ivanov and A. G. Abanov, Phase transitions in full counting statistics for periodic pumping, Europhys. Lett. **92**, 37008 (2010).

[8] F. J. Gómez-Ruiz, J. J. Mayo, and A. del Campo, Full Counting Statistics of Topological Defects after Crossing a Phase Transition, Phys. Rev. Lett. **124**, 240602 (2020).

[9] P. Devillard, D. Chevallier, P. Vignolo, and M. Albert, Full counting statistics of the momentum occupation numbers of the Tonks-Girardeau gas, Phys. Rev. A **101**, 063604 (2020).

[10] V. Eisler, Universality in the Full Counting Statistics of Trapped Fermions, Phys. Rev. Lett. **111**, 080402 (2013).

[11] I. Lovas, B. Dóra, E. Demler, and G. Zaránd, Full counting statistics of time-of-flight images, Phys. Rev. A **95**, 053621 (2017).

[12] I. Klich and L. Levitov, Quantum Noise as an Entanglement Meter, Phys. Rev. Lett. **102**, 100502 (2009).

[13] M. Esposito, U. Harbola, and S. Mukamel, Nonequilibrium fluctuations, fluctuation theorems, and counting statistics in quantum systems, Rev. Mod. Phys. **81**, 1665 (2009).

[14] S. Gustavsson, R. Leturcq, B. Simovič, R. Schleser, T. Ihn, P. Studerus, K. Ensslin, D. C. Driscoll, and A. C. Gossard, Counting Statistics of Single Electron Transport in a Quantum Dot, Phys. Rev. Lett. **96**, 076605 (2006).

[15] V. F. Maisi, D. Kambly, C. Flindt, and J. P. Pekola, Full Counting Statistics of Andreev Tunneling, Phys. Rev. Lett. **112**, 036801 (2014).

[16] T. C. Liebisch, A. Reinhard, P. R. Berman, and G. Raithel, Atom Counting Statistics in Ensembles of Interacting Rydberg Atoms, Phys. Rev. Lett. **95**, 253002 (2005).

[17] N. Malossi, M. M. Valado, S. Scotto, P. Huillery, P. Pillet, D. Ciampini, E. Arimondo, and O. Morsch, Full Counting Statistics and Phase Diagram of a Dissipative Rydberg Gas, Phys. Rev. Lett. **113**, 023006 (2014).

[18] J. Zeiher, R. van Bijnen, P. Schauß, S. Hild, Jae-yoon Choi, T. Pohl, I. Bloch, and C. Gross, Many-body interferometry of a Rydberg-dressed spin Â lattice, Nat. Phys. **12**, 1095 (2016).

[19] A. Öttl, S. Ritter, M. Köhl, and T. Esslinger, Correlations and Counting Statistics of an Atom Laser, Phys. Rev. Lett. **95**, 090404 (2005).

[20] M. Perrier, Z. Amodjee, P. Dussarrat, A. Dareau, A. Aspect, M. Cheneau, D. Boiron, and C. I. Westbrook, Thermal counting statistics in an atomic two-mode squeezed vacuum state, SciPost Phys. **7**, 002 (2019).

[21] S. T. Flammia, D. Gross, Y.-K. Liu, and J. Eisert, Quantum tomography via compressed sensing: error bounds, sample complexity and efficient estimators, New J. Phys. **14**, 095022 (2012).

[22] R. J. Glauber, The quantum theory of optical coherence, Phys. Rev. **130**, 2529 (1963).

[23] P. E. Dolgirev, J. Marino, D. Sels, and E. Demler, Non-gaussian correlations imprinted by local dephasing in fermionic wires, Phys. Rev. B **102**, 100301(R) (2020).

[24] C. Fabre and N. Treps, Modes and states in quantum optics, Rev. Mod. Phys. **92**, 035005 (2020).

[25] M. Walschaers, Non-Gaussian quantum states and where to find them, PRX Quantum **2**, 030204 (2021).

[26] E. Brunner, A. Buchleitner, and G. Dufour, Many-body coherence and entanglement from randomized correlation measurements, Phys. Rev. Res. **4**, 043101 (2022).

[27] P. Naldesi, A. Elben, A. Minguzzi, D. Clément, P. Zoller, and B. Vermersch, Fermionic correlation functions from randomized measurements in programmable atomic quantum devices, arXiv:2205.00981 (2022).

[28] A. Aspect, Hanbury Brown and Twiss, Hong Ou and Mandel effects and other landmarks in quantum optics: From photons to atoms, in *Current Trends in Atomic Physics*, edited by A. Browaeys, T. Lahaye, T. Porto, C. S. Adams, M. Weidemüller, and L. F. Cugliandolo (Oxford University, New York, 2019).

[29] M. Schellekens, R. Hoppeler, A. Perrin, J. V. Gomes, D. Boiron, A. Aspect, and C. I. Westbrook, Hanbury Brown Twiss effect for ultracold quantum gases, Science **310**, 648 (2005).

[30] R. G. Dall, A. G. Manning, S. S. Hodgman, W. RuGway, K. V. Kheruntsyan, and A. G. Truscott, Ideal n-body correlations with massive particles, Nat. Phys. **9**, 341 (2013).

[31] T. Jeltes, J. M. McNamara, W. Hogervorst, W. Vassen, V. Krachmalnicoff, M. Schellekens, A. Perrin, H. Chang, D. Boiron, A. Aspect, and C. I. Westbrook, Comparison of the Hanbury Brown Twiss effect for bosons and fermions, Nature (London) **445**, 402 (2007).

[32] A. Bergschneider, V. M. Klinkhamer, J. H. Becher, R. Klemt, L. Palm, G. Zürn, S. Jochim, and P. M. Preiss, Experimental characterization of two-particle entanglement through position and momentum correlations, Nat. Phys. **15**, 640 (2019).

[33] S. S. Hodgman, R. G. Dall, A. G. Manning, K. G. H. Baldwin, and A. G. Truscott, Direct measurement of long-range third-order coherence in Bose-Einstein condensates, Science **331**, 1046 (2011).

[34] C. Carcy, H. Cayla, A. Tenart, A. Aspect, M. Mancini, and D. Clément, Momentum-Space Atom Correlations in a Mott Insulator, Phys. Rev. X **9**, 041028 (2019).

[35] H. Cayla, S. Butera, C. Carcy, A. Tenart, G. Hercé, M. Mancini, A. Aspect, I. Carusotto, and D. Clément, Hanbury Brown and Twiss Bunching of Phonons and of the Quantum Depletion in an Interacting Bose Gas, Phys. Rev. Lett. **125**, 165301 (2020).

[36] A. Tenart, G. Hercé, J.-P. Bureik, A. Dareau, and D. Clément, Observation of pairs of atoms at opposite momenta in an equilibrium interacting Bose gas, Nat. Phys. **17**, 1364 (2021).

[37] M. Holten, L. Bayha, K. Subramanian, S. Brandstetter, C. Heintze, P. Lunt, P. M. Preiss, and S. Jochim, Observation of cooper pairs in a mesoscopic two-dimensional fermi gas, Nature (London) **606**, 287 (2022).

[38] L. P. Pitaevskii and S. Stringari, *Bose-Einstein Condensation* (Clarendon, Oxford, 2004).

[39] C. Carcy, G. Hercé, A. Tenart, T. Roscilde, and D. Clément, Certifying the Adiabatic Preparation of Ultracold Lattice Bosons in the Vicinity of the Mott Transition, Phys. Rev. Lett. **126**, 045301 (2021).

[40] H. Cayla, C. Carcy, Q. Bouton, R. Chang, G. Carleo, M. Mancini, and D. Clément, Single-atom-resolved probing of lattice gases in momentum space, Phys. Rev. A **97**, 061609(R) (2018).

[41] A. Tenart, C. Carcy, H. Cayla, T. Bourdel, M. Mancini, and D. Clément, Two-body collisions in the time-of-flight dynamics of lattice Bose superfluids, Phys. Rev. Res. **2**, 013017 (2020).

[42] L. Mandel and E. Wolf, *Optical Coherence and Quantum Optics* (Cambridge University, New York, 1995).

[43] K. Laiho, T. Dirmeier, M. Schmidt, S. Reitzenstein, and C. Marquardt, Measuring higher-order photon correlations of faint quantum light: A short review, Phys. Lett. A **435**, 128059 (2022).

[44] S. Fölling, F. Gerbier, A. Widera, O. Mandel, T. Gericke, and I. Bloch, Spatial quantum noise interferometry in expanding ultracold atom clouds, Nature (London) **434**, 481 (2005).

[45] E. Toth, A. M. Rey, and P. B. Blakie, Theory of correlations between ultracold bosons released from an optical lattice, Phys. Rev. A **78**, 013627 (2008).

[46] D. F. Walls and G. J. Milburn, *Quantum Optics* (Springer-Verlag, Berlin, 2008).

[47] See Supplemental Material at http://link.aps.org/supplemental/10.1103/PhysRevResearch.5.L012037 for an analysis of the multimode statistics of Mott insulators, a detailed presentation of the procedures to extract magnitudes of correlation functions, a discussion of the limit on measuring high-order correlations, and a presentation and an analysis of the heuristic model describing the observed deviations in Bose superfluids.

[48] Y. Castin and R. Dum, Low-temperature Bose-Einstein condensates in time-dependent traps: Beyond the $u(1)$ symmetry-breaking approach, Phys. Rev. A **57**, 3008 (1998).

[49] N. I. Akhiezer, *The Classical Moment Problem and Some Related Questions in Analysis*, edited by Oliver Boyd (Dover Publications, Edinburgh, 1965).

[50] D. Contessi, A. Recati, and M. Rizzi, Phase diagram detection via Gaussian fitting of number probability distribution, arXiv:2207.01478 (2022).